Medicinska istraživanja 2025 | DOI: 10.5937/medi0-55068

OPEN ACCESS

Medical Research | Published by Faculty of Medicine University of Belgrade

ORIGINAL ARTICLE

Immunohistochemical and histochemical marker expression in the differential diagnosis of renal cell tumors

Milica Visic[1*], Minya Karac[1*], Maja Zivotic[2], Dusko Dundjerovic[2], Jovan Jevtic[2], Sanja Radojevic-Skodric[2,3], Jelena Filipovic[1]

[1]University of Belgrade, Faculty of Medicine, Belgrade, Serbia

[2]University of Belgrade, Faculty of Medicine, Institute of Pathology, Belgrade, Serbia

[3]Republic Fund of Health Insurance, Belgrade, Serbia

*These two authors contributed equally to this paper

Submitted: 28 November 2024

Revised: 22 September 2025

Accepted: 30 September 2025

Online First: 07 October 2025

Published: 24 December 2025

Check for updates

Correspondence to:
Jelena Filipovic
University of Belgrade, Faculty of Medicine, Institute of Pathology
1 Dr Subotica Street, 11000 Belgrade, Serbia
Email: vjesticaj@gmail.com

Summary

Introduction: The most common renal cell tumors (RCTs) include clear cell renal cell carcinoma (ccRCC), ccRCC with eosinophilic component (ccRCCe), papillary RCC (pRCC), chromophobe RCC (chRCC), and renal oncocytoma (RO). Due to overlapping morphological features, immunohistochemical (IHC) and histochemical (HC) markers are crucial for accurate differential diagnosis.

Materials and Methods: This retrospective study included 237 patients. Tissue microarrays were manually prepared and stained with H&E, CAIX, AMACR, CD10, CD117, CK7, PRMT1, ZEB1, and Hale's colloidal iron. Semiquantitative analysis was performed using a BX53 microscope and scanned with a Leica-Aperio AT2 scanner.

Results: Significant gender differences were observed ($p = 0.0003$), with a higher proportion of males in ccRCC, ccRCCe, and pRCC, while RO was more common in females. Tumor size varied significantly ($p = 0.0041$); ccRCCe tumors were the largest (73.1 mm), and RO the smallest (48.3 mm). Compared to ccRCC, ccRCCe showed lower PRMT1, ZEB1, and CAIX expression and higher CD10 expression. pRCC showed high AMACR expression. RO was strongly positive for PRMT1, ZEB1, and CD117, and negative for CK7, CD10, and Hale's stain. Conversely, chRCC was negative for PRMT1 and ZEB1, but positive for CK7, CD117, and Hale's stain.

Conclusion: The following IHC panel may improve diagnostic accuracy: PRMT1+/ZEB1+/CK7–/Hale– for RO; CK7+/PRMT1–/ZEB1–/Hale+ for chRCC; CAIX+/CD10+/AMACR–/CK7– for ccRCC; and AMACR+ for pRCC. Demographic and clinicopathological differences highlight the importance of integrating clinical parameters into diagnosis and treatment planning.

Keywords: renal cell tumors, IHC staining, PRMT1, ZEB1, differential diagnosis

Cite this article as: Visic M, Karac M, Zivotic M, Dundjerovic D, Jevtic J, Radojevic-Skodric S, Filipovic J. Immunohistochemical and histochemical marker expression in the differential diagnosis of renal cell tumors; Medicinska istraživanja 2025;58(4):219-26; DOI: 10.5937/medi0-55068

INTRODUCTION

Renal cell tumors (RCTs) represent a heterogeneous group of neoplasms, comprising approximately 80% of all primary renal malignancies. The most prevalent malignant subtypes of RCT are clear cell renal cell carcinoma (ccRCC), including ccRCC with an eosinophilic component (ccRCCe), papillary RCC (pRCC), and chromophobe RCC (chRCC). Among these, ccRCC is the most common, accounting for 65-70% of RCTs, followed by pRCC (13-20%) and chRCC (5-7%). Renal oncocytoma (RO), a benign variant, accounts for 6-9% of RCTs (1). Despite distinct macroscopic and histopathological characteristics of each subtype, diagnostic challenges arise when overlapping features are observed or when tissue samples are limited, such as in renal biopsy specimens (2). Recent updates in the WHO classification have introduced additional diagnostic entities and emphasized the role of novel biomarkers in resolving challenging differential diagnoses (3). In such cases, the application of immunohistochemical (IHC) and histochemical (HC) markers is critical for accurate differential diagnosis. Currently, the most commonly utilized and widely accepted IHC markers for distinguishing between ccRCC, ccRCCe, chRCC, pRCC, and RO include CAIX, AMACR, CD10, CD117, CK7, and Hale's colloidal iron HC stain (2-5). This study also investigates the expression of PRMT1 and ZEB1, IHC markers for which limited data exist in the current literature (6-8). Given the variability in marker expression in both the literature and clinical practice, this study examined the expression profiles of these markers in various RCT subtypes, comparing them with available data. Alongside IHC analysis, patient demographics and tumor clinicopathological features were also evaluated. According to recent EAU guidelines, accurate subtyping of renal cell tumors is critical for selecting appropriate treatment strategies and improving patient outcomes (9).

MATERIALS AND METHODS

Patient Characteristics and Tumor Samples

This retrospective study included 237 patients who underwent radical or partial nephrectomy at the Urology Clinic of the University Clinical Center of Serbia between January 1, 2010, and December 31, 2020. The distribution of tumor types in the study population, based on frequency, was as follows: 83 ccRCC, 37 ccRCCe, 27 pRCC, 60 RO, and 30 chRCC. Clinical and pathological parameters of the patients and tumors, including age, gender, and tumor size (largest tumor dimension), were obtained through review of the medical archival records. These characteristics for all 237 patients and different RCT subtypes are presented in **Table 1**. The majority of the cohort consisted of older male patients, with a mean age of 61 years. The largest tumor dimension ranged from 73.1 mm in ccRCCe to the smallest of 48.3 mm in RO.

Pathological Criteria for Evaluation

The cohort included 83 (35.0%) cases of ccRCC, 60 (25.3%) cases of RO, 37 (15.6%) cases of ccRCCe, 30 (12.7%) cases of chRCC, and 27 (11.4%) cases of pRCC. The pathological evaluation of RCT subtypes was based on the fifth edition of the WHO classification of tumors of the urinary system and male genital organs (1). Depending on the RCT subtype, tumor size, nuclear grade, and tumor stage were analyzed. The nuclear grade assessment for ccRCC and pRCC was revised according to the WHO/ISUP 2022 guidelines. According to the updated WHO guidelines, pRCC is no longer classified into Type I and Type II categories (1). Since there are no clear recommendations for the nuclear grading of chRCC, these were not assessed (10). Tumor staging was determined according to the TNM classification of the American Joint Committee on Cancer (AJCC), 8th edition, by reviewing the macroscopic descriptions and representative hematoxylin and eosin (H&E) stained slides (11). Macroscopic pathological descriptions of RO were obtained from the pathological reports.

Tissue Microarray

The tissue microarray (TMA) was manually constructed. Slides stained with H&E were analyzed, and three histologically distinct areas were identified for evaluation. Tissue samples for the microarray were extracted from the selected regions and transferred to a recipient paraffin block using a hollow needle with an inner diameter of 1.2 mm. An additional sample of renal cortex and medulla was randomly collected from each case as a control. Sections of 5 micrometers were cut from the TMA blocks and mounted onto appropriate SuperFrost slides, which were then used for IHC staining. Sections of 5 μm thickness were stained with H&E to confirm the nuclear grade and histological type of each tumor. The slides were examined using a BKS53 light microscope with a DP12-CCD camera (Olympus, Germany) and scanned with a Leica-Aperio AT2 scanner. This study was approved by the Ethics Committee of the Faculty of Medicine, University of Belgrade (29/XII-2, December 27, 2017).

Immunohistochemistry

All TMA sections were deparaffinized at room temperature for 20 minutes and rehydrated in descending concentrations of ethanol. Antigen retrieval was performed by immersing the tissue in citrate buffer (pH 6.0) for 20 minutes in a water bath for PRMT1, ZEB1, CAIX, and CD117, while a Tris-EDTA buffer (pH 9.0) was used for CK7, AMACR, and CD10. Endogenous peroxidase

activity was blocked using 3% H_2O_2 for 10 minutes at room temperature. TMA sections were incubated at room temperature for one hour with the following primary antibodies: PRMT1 (ab92299, Abcam, dilution: 1/200), ZEB1 (HPA027524, Sigma Aldrich, dilution: 1/500), CK7 (OV-TL, Dako, dilution: 1/100), CAIX (H-11, Santa Cruz, dilution: 1/100), AMACR (13-H4, Dako, dilution: 1/200), CD10 (56-C6, Dako, ready-to-use), and CD117 (A4502, Dako, dilution: 1/300). In addition, all slides were stained with Hale's colloidal iron for special HC analysis. The slides were then incubated with Envision in FLEKS/HRP (K4063, Dako, Denmark) for 30 minutes. Staining was visualized by exposure to 3,3′-diaminobenzidine (DAB) and counterstained with Mayer's hematoxylin. Finally, the slides were dehydrated in ethanol, cleared in xylene, and cover-slipped. Human renal tissue was used as the positive control, while the omission of the primary antibody and the use of Tris-buffered saline as a substitute served as the negative control.

Evaluation of IHC and Hale's Colloidal Iron Staining

IHC staining for all markers was evaluated without prior knowledge of patient information or diagnosis. The validity of results was considered as follows: nuclear staining for PRMT1 and ZEB1, membranous staining for CK7, CAIX, CD10, and CD117, cytoplasmic staining for AMACR, and cytoplasmic special staining with Hale's colloidal iron for chRCC and apical membrane staining in RO. A semiquantitative evaluation of IHC staining was performed by determining the percentage of positive tumor cells: 0 (<10%); 1 (11%-25%); 2 (26%-50%); 3 (51%-75%); and 4 (>75%). Staining intensity was rated as follows: 0 (no staining), 1 (weak staining = light yellow), 2 (moderate staining = yellow-brown), and 3 (intense staining = brown). The final staining index (0-12) was calculated by multiplying the extent of positivity by the intensity score. Cases were classified into three groups: no IHC expression (score 0), weak expression (score 1-6), and high expression (score 7-12) (10).

STATISTICAL ANALYSIS

Statistical analysis was conducted using SPSS software (version 20.0). Appropriate statistical methods were applied based on the type of variable. The normality of distribution for continuous variables was assessed using the Shapiro–Wilk test. Depending on the results, either one-way analysis of variance (ANOVA) was used for normally distributed variables or the Kruskal–Wallis test for non-normally distributed variables. Categorical (discrete) variables were analyzed using the chi-square test, and when expected frequencies were below 5, Fisher's exact test was applied. A p-value < 0.05 was considered statistically significant.

RESULTS

Among the analyzed RCTs, statistically significant differences were observed across several clinicopathological parameters. Sex distribution showed a statistically significant difference among tumor types ($p < 0.01$), with a male predominance in ccRCC, ccRCCe, and pRCC, while females were more frequently affected by renal oncocytoma (RO). Tumor size significantly differed between groups ($p = 0.0041$), with the largest tumors seen in ccRCCe and the smallest in RO **(Table 1)**.

The IHC expression data for PRMT1, ZEB1, CK7, CAIX, AMACR, CD10, and CD117 in the most common RCT subtypes, along with special HC staining with Hale's colloidal iron, are presented in **Table 2**, as well as **Figures 1 and 2**. Distinct marker expression and HC staining showed significant associations with RCT subtypes ($p<0.001$). As expected, ccRCC showed the highest predominant expression of CAIX **(Figure 1A)**. In contrast, ccRCCe exhibited weaker CAIX expression relative to ccRCC but displayed a higher proportion of cases with strong CD10 expression **(Figure 1B)**. The majority of ccRCC and ccRCCe cases showed negative PRMT1 and ZEB1 expression, or when positive, the expression was predominantly low. In the case of pRCC, most tumors exhibited prominent AMACR expression **(Figure 1C)**, while CK7 expression in pRCC was notably heterogeneous. RO and chRCC both expressed CD117, while this marker was negative in the remaining RCT types **(Figure 1D-E)**. ChRCC exhibited strong positivity for Hale's colloidal iron staining, while the other tumor subtypes were mostly negative **(Figure 1F)**. RO strongly expressed PRMT1, in contrast to its absence in the majority of chRCC cases **(Figure 2A-B)**. The majority of RO cases exhibited ZEB1 staining with variable intensity, whereas ZEB1 staining was uniformly negative in all chRCC cases **(Figure 2C-D)**. Most RO samples were CK7-negative, while a high IHC positivity for CK7 was observed in the majority of chRCC cases ($p<0.001$) **(Figure 2E-F)**.

DISCUSSION

Morphological similarities among RCTs pose challenges in differential diagnosis. In our study, the sex distribution showed a male predominance in ccRCC, ccRCCe, and pRCC, while RO was more frequently observed in females. This pattern partly aligns with existing literature, as both ccRCC and RO—representing the most common malignant and benign renal tumors, respectively—have typically been reported as more prevalent in males (1). The higher incidence of RO in females in our cohort may reflect population-specific factors such as environmental influences, healthcare access, referral biases, or sample size variation, rather than a fundamental change in tumor biology.

Table 1. Demographic characteristics of patients and clinicopathological parameters of tumors

	Histopathological types of RCT					
	ccRCC	ccRCCe	pRCC	RO	chRCC	Total N (%)
N (%)	83 (35.0%)	37 (15.6%)	27 (11.4%)	60 (25.3%)	30 (12.7%)	237 (100%)
Age, mean ± SD (years)	60 ± 9.5	63 ± 8.6	64 ± 10.0	63 ± 10.1	58 ± 13.4	61 ± 10.7
Sex N(%)						
Male	48 (57.8%)	29 (78.4%)	20 (74.1%)	22 (36.7%)	15 (50.0%)	134 (56.5%)
Female	35 (42.2%)	8 (21.6%)	7 (25.9%)	38 (63.3%)	15 (50.0%)	103 (43.5%)
Tumor size, mean ± SD (mm)	60.9 ± 34.2	73.1 ± 26.8	66.6 ± 22.6	48.3 ± 21.7	67.3 ± 29.4	62.1 ± 29.6
Grade N(%)						
I	18 (21.7%)	1 (2.7%)	3 (11.1%)	NA	NA	22 (15.0%)
II	53 (63.9%)	16 (43.3%)	15 (55.6%)			84 (57.1%)
III	10 (12.0%)	9 (24.3%)	4 (14.8%)			23 (15.6%)
IV	2 (2.4%)	11 (29.7%)	5 (18.5%)			18 (12.3%)
Stage N (%)						
pT1	44 (53.1%)	12 (32.4%)	8 (29.6%)	NA	14 (46.7%)	78 (41.3%)
pT2	10 (12.0%)	4 (10.8%)	4 (14.9%)		4 (13.3%)	22 (11.6%)
pT3	24 (28.9%)	19 (51.4%)	13 (48.1%)		11 (36.7%)	67 (35.4%)
pT4	3 (3.6%)	1(2.7%)	1 (3.7%)		0 (0.0%)	5 (2.6%)
PN	2 (2.4%)	1 (2.7%)	1 (3.7%)	12 (20.0%)	1 (3.3%)	17 (9.1%)

Legend: RCT - renal cell tumors, ccRCC - clear cell renal cell carcinoma,ccRCCe - ccRCC with eosinophilic component, pRCC - papillary RCC,chRCC - chromophobe RCC, RO - renal oncocytoma, N - number, NA - not available, PN - partial nephrectomy, SD - standard deviation

Table 2. Expression of different IHH markers in different types of RCC

Histological Type	ccRCC	ccRCCe	pRCC	RO	chRCC	p value
PRMT1, N (%)						
High expression	19 (22.9%)	3 (8.1%)	8 (29.6%)	47 (78.3%)	2 (6.7%)	<0.001*
Low expression	30 (36.1%)	10 (27.0%)	7 (25.9%)	9 (15.0%)	7 (23.3%)	
No expression	34 (41.0%)	24 (64.9%)	12 (44.5%)	4 (6.7%)	21 (70.0%)	
ZEB1, N (%)						
High expression	1 (1.2%)	0 (0.0%)	1 (3.7%)	28 (46.7%)	0 (0.0%)	<0.001*
Low expression	11 (16.3%)	7 (18.9%)	1 (3.7%)	24 (40.0%)	0 (0.0%)	
No expression	66 (82.5%)	30 (81.1%)	25 (92.6%)	8 (13.3%)	30 (100%)	
CK7, N (%)						
High expression	2 (2.5%)	1 (2.7%)	11 (40.7%)	3 (5.0%)	24 (80.0%)	<0.001*
Low expression	10 (12.3%)	1 (2.7%)	5 (18.6%)	17 (28.3%)	4 (13.3%)	
No expression	69 (85.2%)	35 (94.6%)	11 (40.7%)	40 (66.7%)	2 (6.7%)	
CAIX, N (%)						
High expression	56 (71.8%)	19 (57.6%)	2 (7.4%)	0 (0.0%)	1 (3.3%)	<0.001*
Low expression	19 (24.4%)	7 (21.2%)	5 (18.5%)	0 (0.0%)	1 (3.3%)	
No expression	3 (3.8%)	7 (21.2%)	20 (74.1%)	60 (100%)	28 (93.4%)	
AMACR, N (%)						
High expression	6 (7.6%)	9 (25.7%)	23 (85.2%)	12 (20.0%)	1 (3.3%)	<0.001*
Low expression	19 (24.1%)	9 (25.7%)	3 (11.1%)	27 (45.0%)	2 (6.7%)	
No expression	54 (68.3%)	17 (48.6%)	1 (3.7%)	21 (35.0%)	27 (90.0%)	
CD10, N (%)						
High expression	59 (71.1%)	31 (83.9%)	8 (29.6%)	12 (20.0%)	5 (16.7%)	<0.001*
Low expression	16 (19.3%)	5 (13.4%)	11 (40.8%)	9 (15.0%)	7 (23.3%)	
No expression	8 (9.6%)	1 (2.7%)	8 (29.6%)	39 (65.0%)	18 (60.0%)	
CD117, N (%)						
High expression	0 (0.0%)	0 (0.0%)	0 (0.0%)	33 (55.0%)	17 (56.7%)	<0.001*
Low expression	4 (4.8%)	2 (5.4%)	1 (3.7%)	12 (20.0%)	10 (33.3%)	
No expression	79 (95.2%)	35 (94.6%)	26 (96.3%)	15 (25.0%)	3 (10.0%)	
Hale's colloidal Fe						
High expression	0 (0.0%)	0 (0.0%)	0 (0.0%)	2 (3.3%)	21 (70.0%)	<0.001*
Low expression	3 (3.8%)	4 (11.1%)	4 (14.8%)	9 (15.0%)	5 (16.7%)	
No expression	80 (96.2%)	32 (88.9%)	23 (85.2%)	49 (81.7%)	4 (13.3%)	

Legend: ccRCC - clear cell renal cell carcinoma, ccRCCe - ccRCC with eosinophilic component, pRCC - papillary RCC, chRCC - chromophobe RCC, RO - renal oncocytoma, PRMT1 - protein arginine methyltransferase 1, ZEB1 - Zinc Finger E-Box Binding Homeobox 1, CK7 - cytokeratin 7, CAIX - carbonic anhydrase IX, AMACR - alpha-methyl acyl-CoA racemase, N - number, Fe - iron, *statistically significant p-value

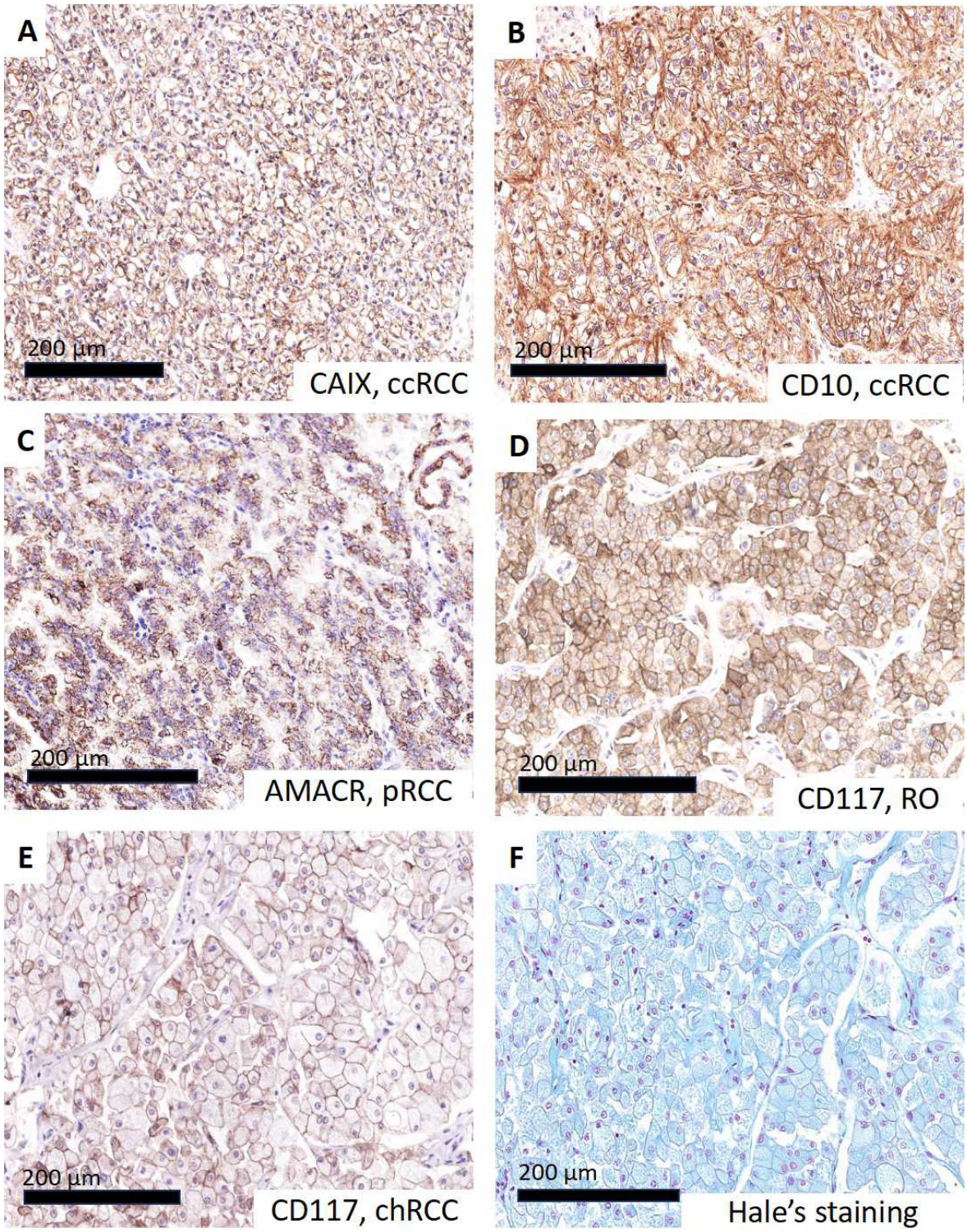

Figure 1. Representative microphotographs illustrate the expression of CAIX, CD10, AMACR, CD117, and Hale's histochemical staining across various RCT types: (A) ccRCC with high membranous CAIX expression; (B) ccRCCe with high membranous and moderate cytoplasmic CD10 positivity; (C) pRCC with strong cytoplasmic AMACR positivity; (D, E) RO and chRCC with high membranous CD117 expression; and (F) chRCC with strong cytoplasmic positivity for Hale's colloidal iron staining: microscope magnification, 200×.

With respect to tumor size, significant differences were observed, with ccRCCe presenting the largest tumors and RO the smallest, consistent with their known biological behavior. This finding suggests that ccRCCe may frequently be diagnosed at more advanced stages, potentially due to its more aggressive nature and tendency to present later in the clinical course (1). Overall, these results highlight the importance of considering both demographic and tumor-specific characteristics in the clinical assessment and management of renal cell tumors. These findings are aligned with the latest European Association of Urology (EAU) Guidelines, which emphasize the importance of integrating tumor size and subtype-specific biology into clinical decision-making and personalized therapeutic strategies (9).

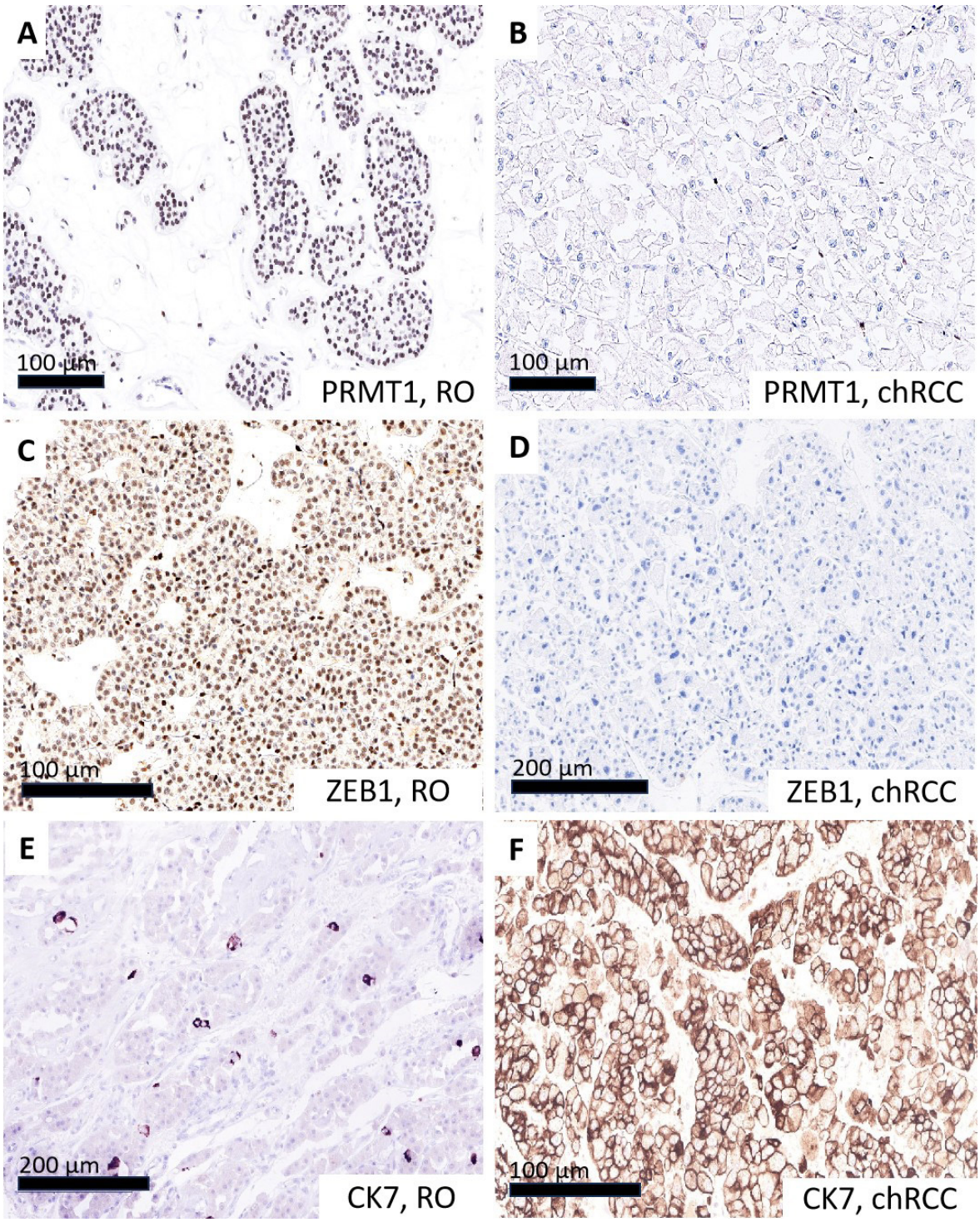

Figure 2. Representative microphotographs of PRMT1, ZEB1, and CK7 expression in RO and chRCC show: (A) high PRMT1 expression in the majority of RO and (B) its absence in most chRCC cases; (C) high nuclear ZEB1 expression in the majority of RO, whereas (D) all chRCC cases were negative for ZEB1; (E) CK7 expression was absent in the majority of RO, while (F) diffuse membranous CK7 staining was present in most chRCC cases: microscope magnification, 100×.

Grossly, ccRCC typically presents as round or oval golden-yellow tumors, often demarcated by a pseudocapsule, with variable necrosis and hemorrhage. Histologically, tumor cells have clear cytoplasm, forming nests, tubular, or alveolar patterns within a rich sinusoidal vascular network. Variants of ccRCC include cystic, hemorrhagic, degenerative, or "scar-like" forms (1). ccRCCe shares features with ccRCC but is distinguished by eosinophilic cytoplasm, more atypia, and frequent necrosis and hemorrhage (4). pRCC is usually well-demarcated, with or without a fibrous capsule, and may be bilateral or multifocal. The cut surface ranges from yellow to red-brown or mixed, depending on the presence of hemorrhage, necrosis, cholesterol, or hemosiderin. High-grade pRCC is solitary and whitish. Histologically, pRCC is characterized by papillary and tubular structures of cuboidal cells with scant cytoplasm, often accompanied by foamy macrophages. Eosinophilic cytoplasm with hemo-

siderin pigment is less common (1). In our experience, low-grade pRCC with simple papillary structures and abundant stroma can resemble RO, creating diagnostic challenges. ROs are well-demarcated, usually non-encapsulated, and red-brown to yellow-brown, often with central scarring. Histologically, they consist of clusters of round to polygonal cells with granular eosinophilic cytoplasm in a myxoid stroma (1). RO variants include forms with chRCC-like features or atypical, bizarre cells, which can present significant challenges in differential diagnosis with chRCC, especially given the increasing number of newly characterized entities and refined diagnostic criteria in the latest WHO classification updates (3, 13-17). ChRCC typically has a solid growth pattern with thin fibrovascular septa and hyalinized blood vessels. Cells show abundant cytoplasm, prominent membranes, pleomorphism, and occasional binucleation. Based on our observations, subtle pleomorphism and prominent vascularization may mimic ccRCC, while chRCC variants with large, bizarre eosinophilic cells can resemble atypical RO (4).

In this study, ccRCCe showed lower expression of PRMT1, ZEB1, and CAIX, and higher CD10 expression compared to ccRCC. These differences may reflect variations in biological behavior, as ccRCCe has been suggested to exhibit more aggressive behavior than pure ccRCC (18,19). Similarly, weak CAIX expression and strong CD10 expression have been reported in sarcomatoid ccRCC, both associated with more aggressive disease (20). Furthermore, lower PRMT1 and ZEB1 expression levels have been linked to shorter survival in ccRCC cases (8). These findings suggest that reduced PRMT1/ZEB1/CAIX and increased CD10 expression may correlate with more aggressive ccRCC forms, particularly in ccRCC with an eosinophilic component.

For pRCC, the key findings included strong AMACR expression, variable CK7 expression, and negative expression of CD117, CAIX, ZEB1, and negative Hale's colloidal iron staining. AMACR showed variable positivity in most RO cases, consistent with Zhu et al., who found AMACR expression in 67% of RO samples (21).

In most RO cases, PRMT1 and ZEB1 were expressed, with PRMT1 frequently showing high intensity, while ZEB1 expression varied in intensity and extent. RO cases were also mostly positive for CD117 and negative for CK7, CD10, and Hale's colloidal iron staining. Conversely, most chRCC cases were negative for PRMT1 and ZEB1, but strongly expressed CK7, CD117, and were positive for Hale's colloidal iron. High CD117 expression in both RO and chRCC, as reported by Zhou et al, suggests that CD117 alone has limited utility in distinguishing between these two entities (22).

CONCLUSION

This study proposes a diagnostic panel of immunohistochemical markers for renal cell tumor subtyping: PRMT1+/ZEB1+/CK7–/Hale's colloidal iron– for RO; CK7+/PRMT1–/ZEB1–/Hale+ for chRCC; CAIX+/CD10+/AMACR–/CK7– for ccRCC; and AMACR+ for pRCC. The use of this combined panel, especially in morphologically ambiguous or limited biopsy samples, may improve diagnostic accuracy and guide further management. Additional research is warranted to characterize ccRCC better and define markers relevant to its diagnosis or prognosis. Furthermore, observed differences in sex distribution and tumor size among RCT subtypes—such as the higher incidence of RO in females and larger tumor size in ccRCCe—highlight the relevance of demographic and clinical parameters in diagnostic and therapeutic planning.

Acknowledgements: N/A

Funding information: This research received no external funding.

Conflicts of interest: The authors declare no conflicts of interest.

Author contributions: All authors contributed to the conception, design, data acquisition, analysis, and interpretation of the study. All authors have read and approved the final manuscript.

Ethical approval: This study was approved by the Ethics Committee of the Faculty of Medicine, University of Belgrade (29/XII-2, December 27, 2017).

Informed consent: Informed consent was obtained from all subjects involved in the study.

References

1. Tateo V, Mollica V, Rizzo A, Santoni M, Massari F. Re: WHO Classification of Tumours, 5th Edition, Volume 8: Urinary and Male Genital Tumours. Eur Urol. 2023;84(3):348-349. DOI: 10.1016/j.eururo.2023.04.030; PMID: 37173211.
2. Bahadoram S, Davoodi M, Hassanzadeh S, Bahadoram M, Barahman M, Mafakher L. Renal cell carcinoma: an overview of the epidemiology, diagnosis, and treatment. G Ital Nefrol. 2022;39(3):2022-vol3. DOI: N/A; PMID:35819037.
3. Sanguedolce F, Mazzucchelli R, Falagario UG, Cormio A, Zanelli M, Palicelli A, Zizzo M, Eccher A, Brunelli M, Galosi AB, Carrieri G, Cormio L. Diagnostic Biomarkers in Renal Cell Tumors According to the Latest WHO Classification: A Focus on Selected New Entities. Cancers (Basel). 2024;16(10):1856. DOI: 10.3390/cancers16101856; PMID: 38791935.
4. Kim M, Joo JW, Lee SJ, Cho YA, Park CK, Cho NH. Comprehensive immunoprofiles of renal cell carcinoma subtypes. Cancers (Basel). 2020;12(3):602. DOI: 10.3390/cancers12030602; PMID: 32150988.
5. Zhu B, Rohan SM, Lin X. Cytomorphology, immunoprofile, and management of renal oncocytic neoplasms. Cancer Cytopathol. 2020;128(12):962-970. DOI: 10.1002/cncy.22330; PMID: 32697415.
6. Sudhakar SRN, Khan SN, Clark A, Hendrickson-Rebizant T, Patel S, Lakowski TM, et al. Protein arginine methyltransferase 1, a major regulator of biological processes. Biochem Cell Biol. 2024;102(2):106-126. DOI: 10.1139/bcb-2023-0212; PMID: 37922507.

7. Sun J, Wang S, Liu P, Liu Y. MiR-139-5p-ZEB1 is a molecular regulator of growth, invasion, and epithelial-to-mesenchymal transition of cervical cancer. Cancer Manag Res. 2020;12:12723-12733. DOI: 10.2147/CMAR.S266167; PMID: 33328767.
8. Filipović J, Bosić M, Ćirović S, Životić M, Dunđerović D, Đorđević D, et al. PRMT1 expression in renal cell tumors - Application in differential diagnosis and prognostic relevance. Diagn Pathol. 2019;14(1):120. DOI: 10.1186/s13000-019-0901-6; PMID: 31655611.
9. Bex A, Ghanem YA, Albiges L, Bonn S, Campi R, Capitanio U, et al. European Association of Urology Guidelines on Renal Cell Carcinoma: The 2025 Update. Eur Urol. 2025;87(6):683–696. DOI: 10.1016/j.eururo.2025.02.020; PMID: 40118739.
10. Cornejo KM, Rice-Stitt T, Wu CL. Updates in Staging and Reporting of Genitourinary Malignancies. Arch Pathol Lab Med. 2020;144(3):305-319. DOI: 10.5858/arpa.2019-0544-RA. PMID: 32101056.
11. Amin MB, Greene FL, Edge SB, Compton CC, Gershenwald JE, Brookland RK, et al. The Eighth Edition AJCC Cancer Staging Manual: Continuing to build a bridge from a population-based to a more "personalized" approach to cancer staging. CA Cancer J Clin. 2019;67(2):93–99. DOI: 10.3322/caac.21388; PMID: 30646056.
12. Yin L, Li W, Xu A, Shi H, Wang K, Yang H, et al. SH3BGRL2 inhibits growth and metastasis in clear cell renal cell carcinoma via activating hippo/TEAD1-Twist1 pathway. EBioMed. 2020;51:102596. DOI: 10.1016/j.ebiom.2019.102596; PMID: 31981375.
13. Hes O, Trpkov K. Do we need an updated classification of oncocytic renal tumors?: Emergence of low-grade oncocytic tumor (LOT) and eosinophilic vacuolated tumor (EVT) as novel renal entities. Modern Pathol. 2022;35(9):1140–1150. DOI: 10.1038/s41379-022-00865-7; PMID: 35819037.
14. Ricketts CJ, De Cubas AA, Fan H, Smith CC, Lang M, Reznik E, et al. The Cancer Genome Atlas Comprehensive Molecular Characterization of Renal Cell Carcinoma. Cell Rep. 2024;43(4):113063. DOI: 10.1016/j.celrep.2023.113063; PMID: 37173211.
15. Bui TO, Dao VT, Nguyen VT, Feugeas JP, Pamoukdjian F, Bousquet G. Genomics of Clear-cell Renal Cell Carcinomas. A Systematic Review and Meta-analysis. Eur Urol. 2022;81(4):349-361. DOI: 10.1016/j.eururo.2021.12.014; PMID: 35027219.
16. Tang H, Xu W, Lu J, Anwaier A, Ye D, Zhang H. Heterogeneity and function of cancer-associated fibroblasts in renal cell carcinoma. J Natl Cancer Cent. 2023;3(2):100-105. DOI: 10.1016/j.jncc.2023.04.001; PMID: 39035728.
17. Characterization of Clear Cell Renal Cell Carcinoma Reveals Prognostic Significance of Epithelial-mesenchymal Transition Gene Expression Signature. Eur Urol Oncol. 2022;5(1):92-99. DOI: 10.1016/j.euo.2021.09.003; PMID: 34692963.
18. Thaib PKP, Rahaju AS. Clinicopathological Profile of Clear Cell Renal Cell Carcinoma. IJHMS. 2022;5(1):91-100. https://doi.org/10.21744/ijhms.v5n1.1846.
19. Nallandhighal S, Vince R, Karim R, Groves S, Stangl-Kremser J, Russel C, et al. Molecular features of renal cell carcinoma. IJHMS. 2022;5(1):91-100. DOI: 10.1016/j.euo.2021.10.007; PMID: 34840106.
20. Nilsson H, Lindgren D, Axelson H, Brueffer C, Saal LH, Lundgren J, et al. Features of increased malignancy in eosinophilic clear cell renal cell carcinoma. J Pathol. 2020;252:384–397. DOI: 10.1002/path.5446; PMID: 31858124.
21. Courcier J, Taille A, Nourieh M, Leguerney I, Lassau N, Ingles A. Carbonic Anhydrase IX in Renal Cell Carcinoma, Implications for Disease Management. Int J Mol Sci. 2020;21(19):7146. DOI: 10.3390/ijms21197146; PMID: 33075888.
22. Zhou J, Yang X, Zhou L, Zhang P, Wang C. Combined immunohistochemistry for the "three markers" (CK7, CD117, and Claudin-7) is useful in the diagnosis of chromophobe renal cell carcinoma and for the exclusion of mimics: Diagnostic experience from a single institution. Dis Markers. 2019;2019:e4708154. DOI: 10.1155/2019/4708154; PMID: 31858124.

ZNAČAJ EKSPRESIJE IMUNOHISTOHEMIJSKIH MARKERA I HISTOHEMIJSKOG BOJENJA U RAZLIČITIM TIPOVIMA TUMORA BUBREŽNIH ĆELIJA

Milica Višić[1], Minya Karac[1], Maja Životić[2], Duško Dunđerović[2], Jovan Jevtić[2], Sanja Radojević-Škodrić[2,3], Jelena Filipović[1]

Sažetak

Uvod: Najčešći bubrežni ćelijski tumori (RCT) uključuju svetloćelijski bubrežni karcinom (ccRCC), ccRCC sa eozinofilnim komponentama (ccRCCe), papilarni RCC (pRCC), hromofobni RCC (chRCC) i renalni oncocitom (RO). Zbog preklapanja morfoloških karakteristika, imunohistohemijski (IHC) i histohemijski (HC) markeri su ključni za tačnu diferencijalnu dijagnozu.

Materijali i metode: Ova retrospektivna studija obuhvatila je 237 pacijenata. Tkivni mikronizovi su ručno pripremljeni i obojeni H&E, CAIX, AMACR, CD10, CD117, CK7, PRMT1, ZEB1 i Hale-ovim koloidalnim gvožđem. Semikvantitativna analiza je izvršena pomoću BX53 mikroskopa i skenirana sa Leica-Aperio AT2 skenerom.

Rezultati: Značajne razlike u distribuciji po polu su uočene (p = 0,0003), sa većim brojem muškaraca u ccRCC, ccRCCe i pRCC grupama, dok je RO bio češći kod žena. Veličina tumora značajno se razlikovala (p = 0,0041); ccRCCe tumori su bili najveći (73,1 mm), a RO najmanji (48,3 mm). U poređenju sa ccRCC, ccRCCe je pokazao nižu ekspresiju PRMT1, ZEB1 i CAIX, ali veću ekspresiju CD10. pRCC je pokazao visoku ekspresiju AMACR. RO je bio jako pozitivan na PRMT1, ZEB1 i CD117, a negativan na CK7, CD10 i Hale-ovo bojenje Suprotno tome, chRCC je bio negativan za PRMT1 i ZEB1, ali pozitivan za CK7, CD117 i Hale-ovo bojenje.

Zaključak: Sledeći IHC panel može pomoći u diferencijalnoj dijagnozi najčešćih tumora bubrega: PRMT1+/ZEB1+/CK7–/Hale– za RO; CK7+/PRMT1–/ZEB1–/Hale+ za chRCC; CAIX+/CD10+/AMACR–/CK7– za ccRCC; i AMACR+ za pRCC. Demografske i kliničko-patološke razlike naglašavaju značaj integracije kliničkih parametara u dijagnozu i planiranje lečenja.

Ključne reči: bubrežni ćelijski tumori, IHC bojenje, PRMT1, ZEB1, diferencijalna dijagnoza

Primljen: 28.11.2024. | **Revidiran:** 22.09.2025. | **Prihvaćen:** 30.09.2025. | **Online First:** 07.10.2025. | **Objavljen:** 24.12.2025.

Medicinska istraživanja 2025